Academic Journal of Science and Technology
ISSN: 2771-3032 | Vol. 5, No. 1, 2023

Dynamic Response Analysis of Buried Aviation Oil Pipeline Under Heavy Vehicle Load

Tao Wang[1], Gen Li[2], Yi Hu[1], Wei Zhu[1], Ziyang Chen[1], Xiaodong Wu[3], Hao Zhang[3]

[1]General Department, China Aviation Oil Pengzhou Pipeline Transportation Co., Ltd, Chengdu, China
[2]China Aviation Oil Group Logistics Co., Ltd
[3]School of Petroleum Engineering, Southwest Petroleum University, Chengdu, China

Abstract: The risk of damage caused by the third party construction such as vehicle rolling is increasing day by day, which seriously threatens the production and operation of the aviation oil pipeline and the life and property safety of the people along the line. Based on the theoretical calculation model of vehicle rolling, the finite element models of pipeline, soil and pipe-soil are established respectively. At the same time, the moving load is loaded using the VLOAD subroutine, and the numerical simulation is carried out using ABAQUS. Finally, the influence of vehicle rolling load on the dynamic response of buried gas pipeline under different vehicle weight and speed conditions is analyzed. The research results have important guiding value for preventing the damage accident of aviation oil pipeline caused by vehicle crushing and guaranteeing the safe and smooth operation of aviation oil pipeline.

Keywords: Heavy vehicle crushing, Loading, Aviation oil pipeline, Finite element analysis.

1. Introduction

China's existing aviation oil pipelines are mostly planned and constructed around large and medium-sized cities, which generally pass through multiple jurisdictions of the cities and often cross several roads of different grades, including national roads, provincial roads and various township roads. With the rapid development of urbanization and the gradual replenishment of satellite cities, the environment around the aviation oil pipeline, which was originally located in the suburban area, has changed dramatically, and the production and construction activities around the pipeline have become more frequent, and the number of temporary construction roads intersecting with the pipeline has increased, so that the risk of third-party construction damage such as vehicle crushing has increased day by day (Shuyi et al., 2022). The aviation oil pipeline designed and constructed in the early stage may not have additional protection measures such as casing and cover culvert at the new road, in this case the aviation oil pipeline will be frequently crushed by construction vehicles which will lead to continuous settlement of the foundation around the pipeline, once the allowable stress-strain value is exceeded, it will have a non-negligible impact on the pipeline and seriously threaten the production and operation of the aviation oil pipeline and the safety of people's lives and properties along the route. In addition, due to the special nature of the jet fuel pipeline, it will also cause airport grounding and bring great negative impact to the ecological environment, social stability and public safety along the pipeline (Liu Dong, 2007). Therefore, it is particularly important to analyze the impact of vehicle crushing on buried aviation oil pipelines and to determine effective protective measures for pipelines to ensure safe and reliable operation of aviation oil pipelines.

2. Theoretical Calculation of Heavy Vehicle Load

At present, domestic and foreign in the design work of the aviation oil pipeline crossing the road is still the vehicle crush load as static load to calculate, the realization of the vehicle dynamic load is used static load multiplied by the corresponding impact coefficient calculation method (CSA, 2014). When the burial depth of the jet fuel pipeline is large, the Boussinesq method is usually used; when it is buried shallow, the distribution angle method is usually used.

2.1. Boussinesq method

Boussinesq method is to consider the load generated by the vehicle crushing as a concentrated force additional load, and to calculate the transfer of load in the soil body according to the elastic theory listed. For any point M (x, y, z) inside the soil body (shown in figure 1), the stresses and displacements are calculated using the Boussinesq method as shown in equation (1) and equation (2) (Gu Xiaolu et al., 2003).

$$\left.\begin{aligned}\sigma_x &= \frac{3Q}{2\pi}\left\{\frac{x^2 z}{R^5}+\frac{1-2\mu}{3}\left[\frac{R^2-Rz-z^2}{R^3(R+z)}-\frac{x^2(2R+z)}{R^3(R+z)^2}\right]\right\}\\ \sigma_y &= \frac{3Q}{2\pi}\left\{\frac{y^2 z}{R^5}+\frac{1-2\mu}{3}\left[\frac{R^2-Rz-z^2}{R^3(R+z)}-\frac{x^2(2R+z)}{R^3(R+z)^2}\right]\right\}\\ \sigma_z &= \frac{3Q}{2\pi}\frac{z^3}{R^5}=\frac{3Q}{2\pi R^2}\cos^3\theta\end{aligned}\right\} \quad (1)$$

Where σ_x , σ_y , σ_z is the normal stresses in x,y,z directions respectively, u,v,w is the displacements of the point M along the coordinate axis (x, y, z), respectively, Q is the vertical concentrated force acting at the origin of the coordinates, E is the deformation modul us of the soil, μ is poisson's ratio of the soil, and R is the directional diameter of point M, $R=\sqrt{x^2+y^2+z^2}=\sqrt{r^2+z^2}$.

$$\left.\begin{aligned} u &= \frac{Q(1+\mu)}{2\pi E}\left[\frac{xz}{R^3}-(1-2\mu)\frac{x}{R(R+z)}\right] \\ v &= \frac{Q(1+\mu)}{2\pi E}\left[\frac{yz}{R^3}-(1-2\mu)\frac{y}{R(R+z)}\right] \\ w &= \frac{Q(1+\mu)}{2\pi E}\left[\frac{z^2}{R^3}+2(1-\mu)\frac{1}{R}\right] \end{aligned}\right\} \quad (2)$$

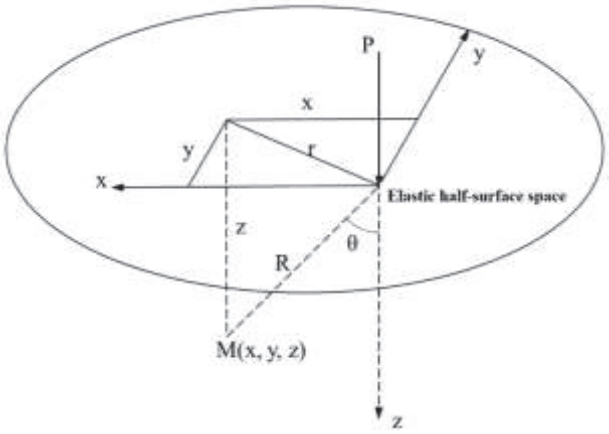

Figure 1. Additional stress in the soil caused by concentrated wheel pressure.

As can be seen from the equation (1), when R tends to 0, M point of stress tends to infinity, that is, the concentration of force near the point of action has produced plastic deformation, so Boussinesq method is not applicable to the pipeline buried in shallow conditions.

Suppose the vehicle grounding wheel track is rectangular, the length and width are a and b, respectively, and the tire grounding stress is p. According to the calculus theory, it can be known that the grounding wheel track coordinates N (x, y) at the peripheral micro-element $dxdy$ on the uniform wheel pressure can be converted into a concentrated force $dF = pdxdy$, then the concentrated force caused by the wheel track center directly below a depth z at the vertical direction of the stress as shown in equation (3).

$$d\sigma_z = \frac{3}{2\pi}\frac{pz^3}{\left(x^2+y^2+z^2\right)^{5/2}}dxdy \quad (3)$$

The integration yields equation (4).

$$\sigma_z = \iint d\sigma_z = 4\times\frac{3p}{2\pi}\int_0^{b/2}\int_0^{a/2}\frac{z^3}{\left(x^2+y^2+z^2\right)^{5/2}}dxdy = 4K_0 p \quad (4)$$

where,

$$K_0 = \frac{1}{\pi}\left[\frac{2abz\left(a^2+b^2+8z^2\right)}{\left(a^2+4z^2\right)\left(b^2+4z^2\right)\sqrt{a^2+b^2+4z^2}}+\arctan\frac{ab}{2z\sqrt{a^2+b^2+4z^2}}\right],$$

is called the corner point stress factor (vertical direction) for rectangular distributed loads.

Existing studies and experiments have shown that when the pipe burial depth is greater than 1m, Boussinesq method has a fairly high reliability, but for pipes with larger diameter and shallow burial depth, the error is larger and should not be used (O C Young et al., 1984).

2.2. Distribution angle method

The distribution angle method is to transfer the ground vehicle crushing load according to the edge of the tire landing area downward at a certain diffusion angle (the value range is 25°~ 45°), and assumes that the vehicle wheel pressure is uniformly distributed in the pipe top plane (Shao Yu, 2002). The Code for Structural Design of Water Supply and Drainage Pipes (GB50332-2002) uses the distribution angle method to calculate the standard value of vertical pressure transmitted by ground vehicle loads to the top of buried pipes.

(1) Single wheel pressure

The standard value of vertical pressure transferred from a single wheel pressure to the top of the pipe is calculated according to equation (5), and the transfer distribution is shown in figure 2 (a) and figure 2 (b).

$$q_{vk} = \frac{\mu_d Q_{vi,k}}{\left(a_i+1.4H\right)\left(b_i+1.4H\right)} \quad (5)$$

Where q_{vk} is the standard value of vertical pressure transmitted by the wheel pressure to the top of the pipe (kN/m^2), $Q_{vi,k}$ is the standard value of the individual wheel pressure borne by i wheels of the vehicle (kN), a_i is the length of the landing distribution of i wheels (m), b_i is the width of the landing distribution of i wheels (m), and H is the depth from the ground of the car line to the top of the pipe (m), and μ_d is the power coefficient, which can be selected according to Table 1.

Table 1. Table of power coefficients.

Length of ground from top of pipe (m)	0.25	0.30	0.40	0.50	0.60	≥0.70
Power factor	1.30	1.25	1.20	1.15	1.05	1.00

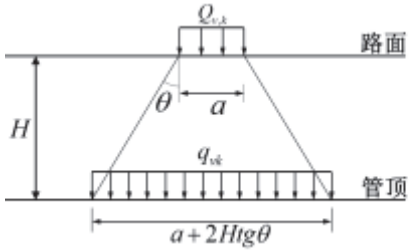

(a) Diagram of the load distribution in the direction of tire length

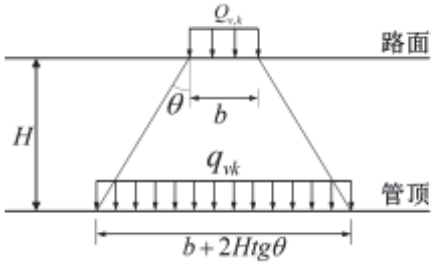

(b) Diagram of the load distribution in the direction of tire width

Figure 2. Diagram of the load distribution in the direction of tire length and width

(2) Single row multiple wheel press

The standard value of the vertical pressure transmitted to the top of the pipe by the combined effect of two or more single-row wheel pressures can be shown in equation (6) (Zhu YT et al., 2015).

$$q_{vk}=\frac{\mu_d n Q_{vi,k}}{\left(a_i+1.4H\right)\left(nb_i+\sum_{j=1}^{n-1}d_{bj}+1.4H\right)} \quad (6)$$

Where n is the total number of single-row wheels, and d_{bj} is the net distance between two adjacent wheels along the direction of the width of the wheel landing distribution (m). Other letters have the same meaning as before.

(3) Multiple rows of multiple wheel presses

The standard value of vertical pressure transmitted to the top of the pipe by the combined effect of multiple rows of wheel pressure can be calculated according to the equation (7).

$$q_{vk}=\frac{\mu_d\sum_{i=1}^{n}Q_{vi,k}}{\left(\sum_{i=1}^{m_a}a_i+\sum_{j=1}^{m_a-1}d_{aj}+1.4H\right)\left(\sum_{i=1}^{m_b}b_i+\sum_{j=1}^{m_b-1}d_{bj}+1.4H\right)} \quad (7)$$

Where m_a is the number of wheel rows along the width of the wheel landing distribution,m_b is the number of rows of wheels along the length of the wheel landing distribution, and d_{bj} is the clear distance between two adjacent wheels along the length of the wheel landing distribution (m).Other letters have the same meaning as before.

2.3. Impact factor

The impact coefficient is the ratio of the measured vertical earth pressure at the top of the pipe to the pressure value calculated according to the static load theory, which reflects the difference between the dynamic and static loads (Deng Daoming et al., 1998). The national code "Code for Structural Design of Water Supply and Drainage Pipelines" (GB50332-2002) also refers to the impact coefficient as the dynamic coefficient, and the range of values is shown in Table 1. For pipelines crossing highways, the impact coefficient is related to factors such as road conditions, vehicle speed, and vehicle type. The British Code for the Design of Rigid Buried Pipelines considers "heavy" loads to be 1.25, "light" loads to be 1.5, and field loads to be 2.0. It is generally accepted that the value of the impact factor ranges from 1 (for rigid pavements) to 1.5 (for unpaved The impact factor is generally considered to range from 1 (for rigid pavements) to 1.5 (for unpaved flexible pavements).

Although these calculation methods are simple and easy to use, they all use the soil medium as a homogeneous elastomer to calculate the vertical action of the vehicle crush load on the top of the buried pipe, and do not consider the influence of the buried pipe on the transfer of stress in the soil, resulting in some deviations between the calculation results and the actual situation (Wang Zemin, 2006).

3. Finite Element Simulation of Heavy Vehicle Crush Test

3.1. Soil model parameters

The M-C model is an ideal elasto-plastic model that integrates Hooke's law and Coulomb's damage criterion, which can well describe the damage behavior of soil and is widely used (Pan Xinmei et al., 2015).The controlling equation of the yield criterion of the M-C model is as follows equation (8) is shown.

$$f=\frac{1}{2}\left(\sigma_1-\sigma_3\right)+\frac{1}{2}\left(\sigma_1+\sigma_3\right)\sin\phi-c\cos\phi=0 \quad (8)$$

Where σ_1 σ_2 , σ_3 is the first, second and third principal stresses (Pa), c is the cohesion (Pa), and ϕ is the angle of internal friction (°).

However, the M-C model assumes that the stress-strain relationship of the soil before reaching shear strength satisfies Hooke's law, and thus does not better reflect the pre-deformation behavior of the soil (Huang F, 2012). the graph of the M-C yield surface in the stress space π-plane is a hexagon with unequal angles, as shown in figure 3. the intersection of each edge on the M-C yield surface is a corner, which also becomes the yield surface singularity of the function, and there are difficulties in calculating the flow vector. To solve this problem, Drucker and Prager changed the yield surface of the M-C criterion in the π-plane to a smooth surface to make it easier for the program to calculate. this criterion is called the D-P criterion, and the model that adheres to this criterion is also called the D-P model. the graph of the D-P criterion in the π-plane is the inner tangent circle or outer circle of the M-C yield curve. the expression of the D-P model is shown in equation (9) .

$$f=\sqrt{J_2}+\alpha I_1-k=0 \quad (9)$$

$$J_2 = \frac{1}{2} s_{ij} s_{ij} \tag{10}$$

$$I_1 = \frac{1}{3} \sigma_{kk} \tag{11}$$

Where s_{ij} is the second stress bias invariant, σ_{kk} is the first stress bias invariant, and α , k is cohesion c and the constant determined by the angle of internal friction (ϕ) .

$$\alpha = \frac{2\sin\phi}{\sqrt{3}\left(3-\sin\phi\right)} \tag{12}$$

$$k = \frac{6c\cos\phi}{\sqrt{3}\left(3-\sin\phi\right)} \tag{13}$$

In this paper, the D-P model is selected for the soil model. The soil parameters selected in this paper are shown in Table 2 and Table 3.

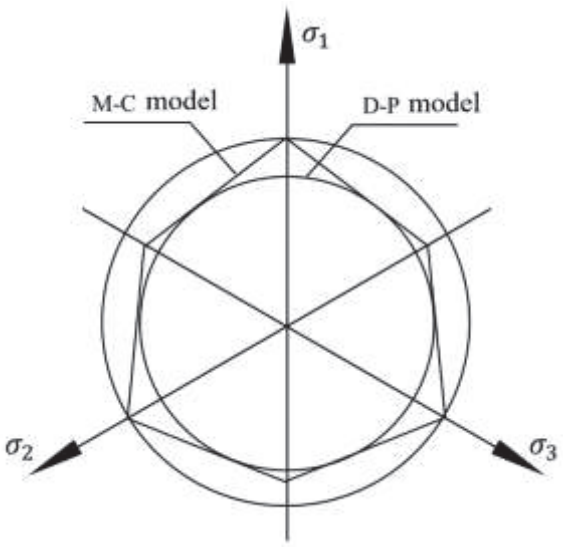

Figure 3. Yield surfaces corresponding to different yielding criteria in the π-plane.

Table 2. Table of soil parameters.

Category	Elasticity parameters			D-P model parameters		
	Density/(kg/m^3)	Modulus of elasticity/MPa	Poisson's ratio	Friction angle/°	Rheological stress ratio	Expansion angle/°
Backfill	1780	14.4	0.4	36	1	0

Table 3. Hardening parameters of D-P model.

Yield stress/MPa	0.17	0.65	0.75	0.8	0.85
Absolute plastic strain	0	0.035	0.051	0.073	0.092

3.2. Pipeline model parameters

In this paper, L360 pipeline steel, which has been applied in aviation oil pipeline in recent years, is selected to analyze the dynamic response of the pipeline under vehicle crushing load. The pipeline material parameters are shown in Table 4.

Table 4. Table of pipe material parameters.

Category	Density (kg/m^3)	Modulus of elasticity/GPa	Poisson's ratio
X70	7850	210	0.3

The linear elastic material model is chosen for the pipe principal structure model, and the relationship of the linear elastic model is shown in equation (14).

$$\sigma = E\varepsilon \tag{14}$$

Where σ is the material stress (Pa), E is the modulus of elasticity of the material (Pa), and ε is the material strain.

The pipe model is a homogeneous model that obeys the Von-Mises yield criterion, which can accurately describe the strength and deformation of steel pipes under dynamic impact.

$$f = \frac{3}{2}\left(s_{ij}-\alpha_{ij}\right)\left(s_{ij}-\alpha_{ij}\right) - \sigma_y \tag{15}$$

Where s_{ij} is the deflective stress tensor, α_{ij} is the back stress tensor, and σ_y is the Yield stress (Pa).

The dynamic yielding criterion can better describe the yielding behavior of the pipe when subjected to impact loading, where the J-C model is an ideal thermo-viscoplastic strengthening model that responds to the strain rate strengthening effect, and its intrinsic model is shown in equation (16) (Zhao Lu, 2018).

$$\sigma = \left[A + B\left(\bar{\varepsilon}^{pl}\right)^n\right]\left[1 + C\ln\left(\varepsilon / e_0\right)\right]\left(1-\theta^m\right) \tag{16}$$

Where $\bar{\varepsilon}^{pl}$ is the equivalent plastic strain of the material, A is the Yield strength at reference strain rate (Pa), B is the strain hardening factor, C is the strain rate hardening factor, and m , n is the material parameters measured lower than the transition temperature.

Let the current temperature of the material be θ ; the melting temperature be θ_m ; and the transition temperature, i.e., the maximum temperature that does not affect the yield stress, be θ_t . Then we have, when $\theta < \theta_t$, $\theta = 0$; when $\theta_t \le \theta \le \theta_m$, $\theta = (\theta - \theta_t)/(\theta_m - \theta_t)$; when $\theta > \theta_m$, $\theta = 0$.

Because the general room temperature will not exceed the transition temperature, equation (16) can be simplified as follows

$$\sigma = \left[A + B\left(\bar{\varepsilon}^{pl}\right)^n \right]\left[1 + C\ln\left(\varepsilon / e_0\right)\right] \quad (17)$$

3.3. Finite element modeling

Assuming that the soil is isotropic and homogeneous continuum, the soil is 21m long, 12m wide and 5m thick along the direction of vehicle travel; according to the field experience of domestic pipeline companies, the model sets the pipeline burial depth at 1m, pipe diameter at 813mm, wall thickness at 11.9mm and gas transmission pressure at 6MPa, and the geometric model diagram of the pipeline and soil is shown in figure 4.

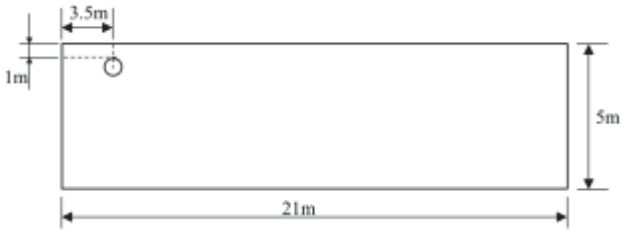

Figure 4. Geometric dimension diagram.

The middle part of the model is set to finite element mesh, and the surrounding and bottom part are set to infinite element mesh. The surface-to-surface contact is used between the pipe and the soil, and the contact surface is set to "hard contact" in the normal direction, and the tangential direction is constrained by a penalty function with a friction coefficient of 0.4. In order to improve the calculation accuracy of the model, the soil cells around the pipeline are encrypted; at the same time, the grid of cells farther away from the pipeline is loosened, which improves the calculation speed of the model. The finite element model is shown in figures 5 (Liao Liao et al., 2017).

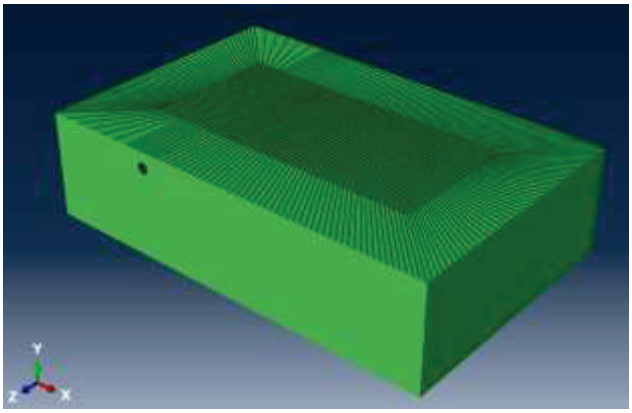

Figure 5. Finite element model diagram.

4. Buried Aviation Oil Pipeline Bearing Capacity Analysis

In this paper, the vehicle crush load is loaded using the VDLOAD subroutine, and the wheel forces of each wheel of the vehicle obtained using the multi-body dynamics simulation as the input values for analyzing the dynamic response model of the pipeline in ABAQUS, which makes up for the lack of taking into account the mobility and dynamics of the vehicle crush load in the existing study.

4.1. Dynamic response analysis

The dynamic response analysis in this paper uses the pipe-soil model established in the previous section, with the internal pressure of the pipe set to 6 MPa and the burial depth set to 1 m. The peak pressure corresponding to the wheel force is loaded at the position directly above the pipe, and the corresponding vehicle crush load condition analysis is carried out. After the analysis, the Mises stress cloud diagram at the moment of maximum stress of the pipe is selected, as shown in figure 6 - figure 9. As can be seen from the figure, when the vehicle travels over the pipe, the maximum Mises stress point of the pipe is not at the position directly below the wheel, but is located near the midpoint of the vehicle wheelbase, where the pipe is subject to the superposition of the downward displacement of the pipe section along both sides of the axial direction, resulting in the maximum stress; the maximum Mises stress value of the pipe is positively correlated with the weight of the vehicle, that is, the greater the weight of the vehicle, the greater the maximum Mises stress value of the pipe response.

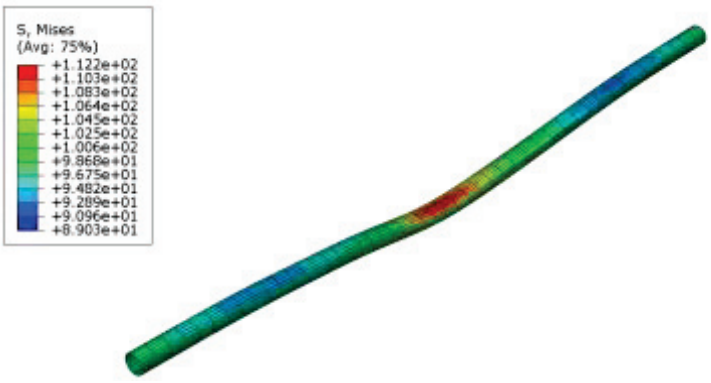

Figure 6. Maximum Mises stress cloud of the pipe with a vehicle weight of 19t and a vehicle speed of 10km/h (max: 112.2MPa).

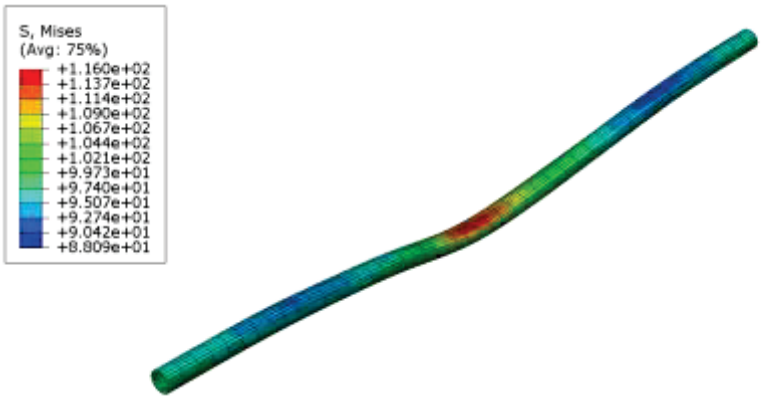

Figure 7. Maximum Mises stress cloud of the pipe with a vehicle weight of 30t and a vehicle speed of 10km/h (max: 116.0MPa).

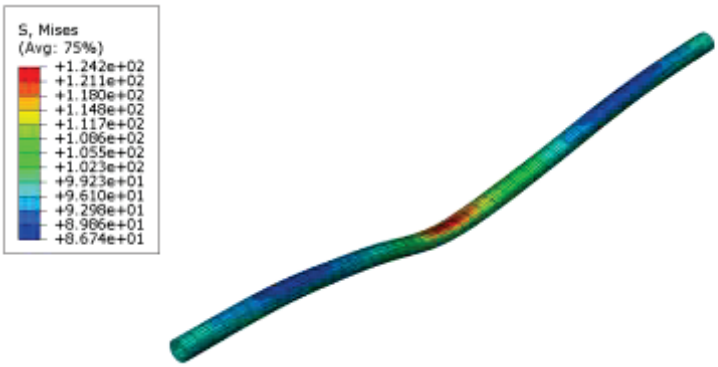

Figure 8. Maximum Mises stress cloud of pipe with 40t vehicle weight and 10km/h vehicle speed (max: 124.2MPa).

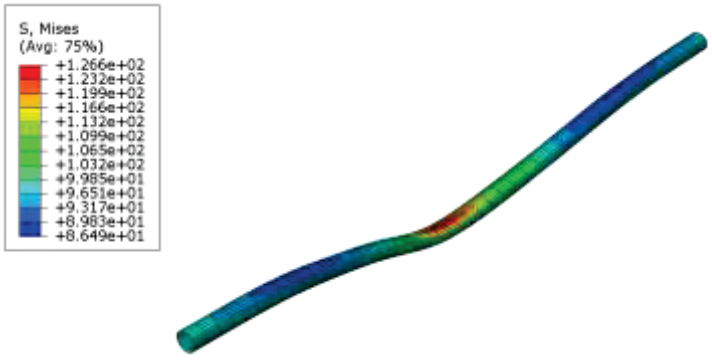

Figure 9. Vehicle weight 50t, speed 10km/h pipe maximum Mises stress cloud (max: 126.2MPa).

At the end of the analysis, the Mises stress clouds at the moment of maximum stress of the pipe for different vehicle speeds were selected simultaneously, as shown in figure 10 - figure 12. The maximum Mises stress value and displacement of the pipe and the vehicle speed are negatively correlated, i.e., the smaller the vehicle speed, the larger the maximum Mises stress value and the larger the strain of the pipe.

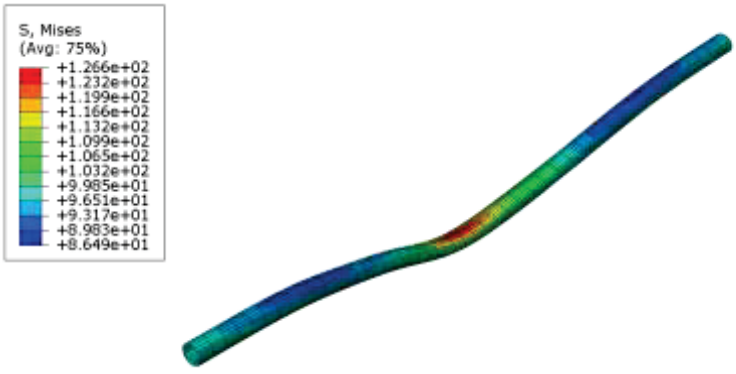

Figure 10. Vehicle weight 50t, speed 10km/h pipe maximum Mises stress cloud (max: 126.2MPa).

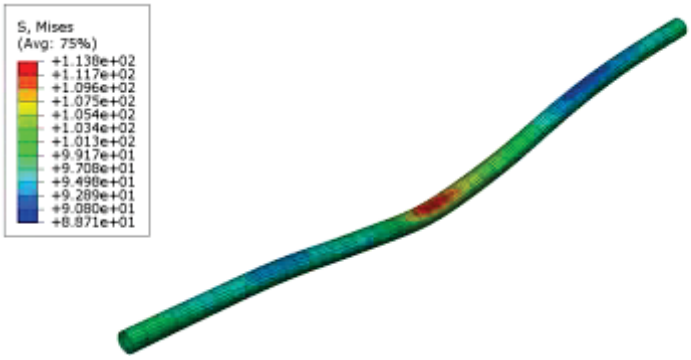

Figure 11. Maximum Mises stress cloud of the pipe with a vehicle weight of 50t and a vehicle speed of 15km/h (max: 113.8MPa).

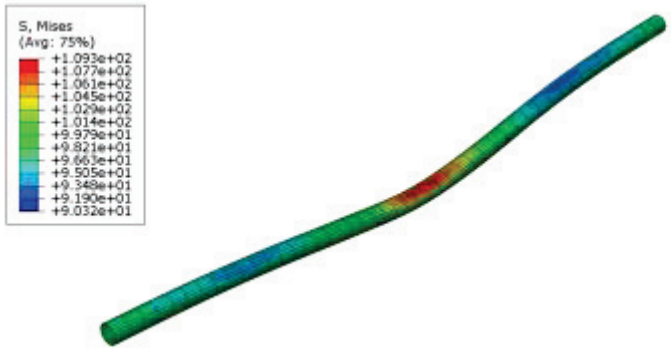

Figure 12. Vehicle weight 50t, speed 20km/h pipe maximum Mises stress cloud (max: 109.3MPa)

The analysis of vertical displacement along the pipeline under different working conditions is shown in figure 13 and figure 14, which shows that the vertical displacement of the pipeline under different working conditions is similar and parabolic downward; when the vehicle drives through the pipeline, the maximum vertical displacement along the pipeline is not at the position directly below the wheels, but is located near the midpoint of the vehicle wheelbase, where the pipeline is subject to the superposition of downward displacement along the axial sides of the pipe section When the vehicle weight increases from 19t to 50t, the maximum vertical displacement of the pipe increases from 3.081mm to 5.897mm, an increase of 2.816mm, an increase of 191.40%; the vertical displacement of the pipe is negatively related to the vehicle speed, the greater the driving speed of the vehicle, the smaller the displacement of the pipe. The displacement of the response is smaller. When the vehicle speed increases from 10km/h to 20km/h, the maximum vertical displacement of the pipe decreases from 5.897mm to 2.552mm, decreasing by 3.345mm, with a reduction rate of 43.28%.

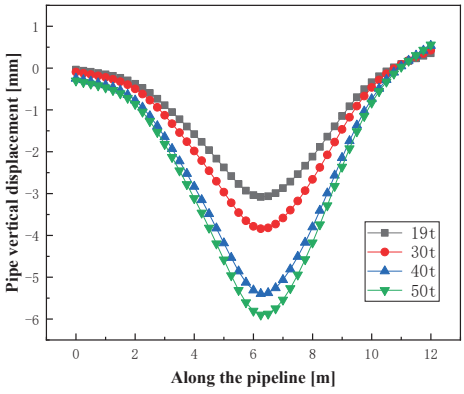

Figure 13. Vertical displacement curves of pipes under different vehicle weight conditions (10km/h - 6MPa-1m).

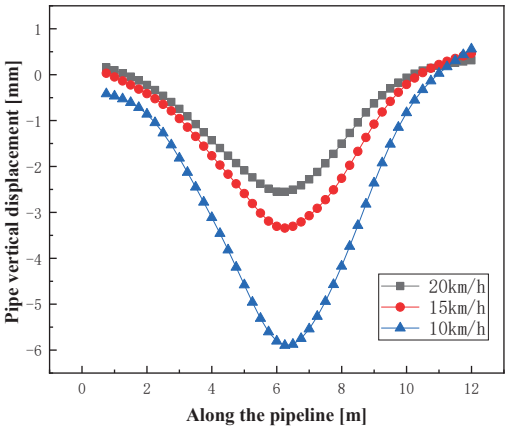

Figure 14. Vertical displacement curves of pipes under different vehicle speed conditions (50t-6MPa-1m).

In order to study the dynamic response process of buried gas transmission pipeline under vehicle crushing load, the Mises stress and displacement response time profile of the pipeline under the working condition of vehicle weight 50t and vehicle speed 10km/h is extracted as figure 15. From the analysis of the figure, it can be seen that the displacement change of the pipeline is mainly divided into three stages when the vehicle travels over the pipeline overburden.

The first stage, 0~0.3s, at this time, the front wheels of the vehicle have not reached the top of the pipe, and the vehicle crushing load has not been transferred to the pipe, the pipe under the joint action of only the internal pressure and the pipe-soil contact occurs stable displacement, the displacement amount is 0.15mm, the stress value also fluctuates little, about 2.12MPa.

The second stage, 0.3s~5.81s, when the vehicles have all passed over the pipe, the stresses and displacements of the

pipe occur once when the front row of wheel forces are transferred to the pipe, reach the first peak at 0.45s, then fall back, and grow and fall back again when the second and third rows of wheels pass by, and have a maximum value when the third row of wheel forces are transferred to the pipe.

The third stage, 5.81s~7.3s, when the vehicle has completely driven away from the top of the pipe, and the stress and displacement of the pipe have started to fall back.

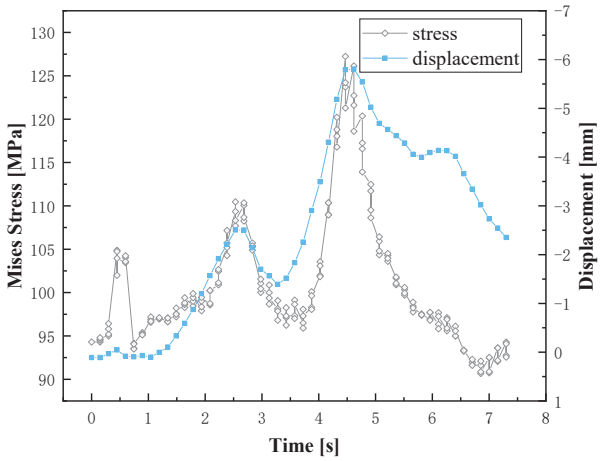

Figure 15. Time response curves of Mises stress and displacement of pipeline (50t-10km/h-6MPa-1m).

4.2. Maximum stress cross-sectional properties

In order to analyze the mechanical characteristics of the buried gas pipeline under the current working condition of vehicle crushing load, the unit on the cross-section of the pipeline at the maximum force is selected and the Mises stress variation diagram of the pipeline is drawn, as shown in figure 16. By analyzing the mechanical properties of the cross-section of the pipeline, it can be seen that when the vehicle runs over the top of the pipeline cover, the stress of the pipeline is greatest in the upper side of the direction of the vehicle, i.e. 300°~15° area in the figure, and this location is the most vulnerable point of the pipeline. The Mises stress in the area of 105°~180°opposite to it is the smallest. The values of Mises stresses in the two side cells are approximately equal and symmetrical.

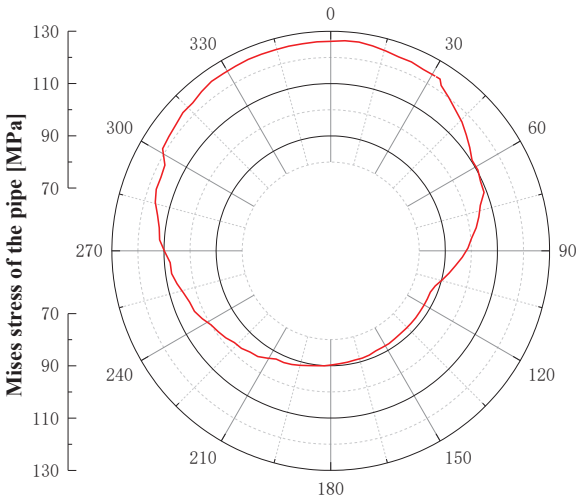

Figure 16. Schematic diagram of stress variation in the maximum stressed cross-section of the pipe.

The deformation diagram of the pipe is shown in figure 17. From the analysis of the diagram, it can be seen that when the vehicle drives over the pipe from left to right, the overall position of the pipe moves down to the right under the vehicle crushing load, and the deformation of the lower right side of the pipe is larger.

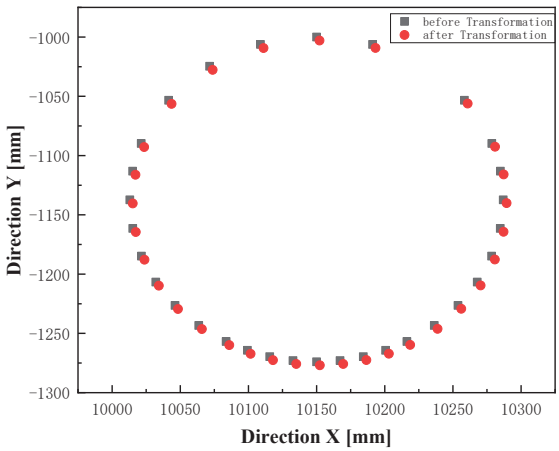

Figure 17. Maximum force cross-sectional deformation of the pipe.

5. Conclusion

In this paper, the finite element models of pipeline, soil and pipe-soil were established respectively, the moving loads were loaded using the VLOAD subroutine, and numerical simulations were carried out using the ABAQUS/Explicit module, and finally the influence law of the vehicle crushing load on the dynamic response of buried gas transmission pipeline under different vehicle weight and different vehicle speed conditions was analyzed, and the following conclusions were drawn.

(1) The finite element model of pipe-soil interaction was established by using ABAQUS software, and the loading of dynamic load was realized by using VLOAD subroutine, taking into account the dynamicity of vehicle crushing load, mobility and wheel rectangular imprint, which effectively solved the problem of low accuracy of traditional vehicle crushing load simulation method.

(2) The maximum Mises stress point and the maximum displacement point of the pipe are located near the midpoint of the vehicle wheelbase, where the pipe is subject to the superposition of the downward displacement of the pipe sections along both sides of the axial direction, resulting in the maximum stress and the maximum displacement; the increase of the vehicle weight will lead to the increase of the maximum Mises stress and the maximum displacement of the pipe response; and with the increase of the vehicle speed, the Mises stress and the maximum displacement generated by the pipe will decrease.

(3) The moment of dynamic response of the pipe is later than the moment when the wheels drive over the pipe; the analysis of the mechanical characteristics of the pipe shows that the Mises stress and displacement on the upper side of the pipe facing the direction of the approaching vehicle are the largest, which is the most vulnerable area of the pipe.

References

[1] CSA S6-14. Canadian Highway Bridge Design Code Buried Structures: Section 7-Buried Structures [S]. CSA, 2014.

[2] Deng Daoming, Wu Bin, Li Yu-Guang. Load calculation for buried pipelines crossing highways [J]. Oil and Gas Storage and Transportation, 1998, (4): 26-31.

[3] Gu Xiaolu, Qian Hongjin, Liu Huishan, etc. Foundations and Foundations (3rd edition) [M]. Beijing: China Construction Industry Press, 2003.

[4] Huang F. Analysis of the impact of metro shield method construction on adjacent pile foundation [D]. Guangzhou University, 2012.

[5] Li Shuyi, Ma Bin, Song Jie et al. Safe burial depth and protective measures for gas transmission pipelines under the action of vehicle crushing [J]. Gas and Thermal Power, 2022, 40(2): 35-38.

[6] Liao Liao, Huang Kun, Wu Jin, Chen Liqiong, Lu Yiqiu. ABAQUS-based mechanical property analysis of gas transmission pipelines crossing highways[J]. China Science and Technology of Safety Production,2017,13(5): 62-68.

[7] Liu Dong. Analysis on the service life and safety management mode of aviation oil long-distance pipeline[J]. Civil Aviation Science and Technology, 2007, (1): 100.

[8] O C Young, J J Trott. Buried Rigid Pipes: Structural Design of Pipelines [M]. London and New York: Elsevier Applied Science Publishers, 1984.

[9] Pan Xinmei, He Keqiang, Li Wei. Numerical simulation analysis of deformation laws of foundation pits supported by different prestressed anchors with composite soil nails [J]. Engineering Construction, 2015, (3): 12-16.

[10] Shao Yu. Failure mechanism of buried pipelines and their reliability [D]. Zhejiang. Zhejiang University. 2002.

[11] Wang Zemin. Study on mechanical properties of buried pipelines under traffic load[D]. Zhejiang University, 2006.

[12] Zhao Lu. Dynamic response and limit analysis of buried gas transmission pipeline under the impact of falling rocks [D]. Southwest Petroleum University,2018.

[13] Zhu YT, Geng YS, Ma Shujiang. Key technologies for ultra-large-diameter long-distance HDPE water transmission pipeline engineering [M]. Beijing: China Water Conservancy and Hydropower Press, 2015.